



Document No: ERS2-GO-DDS-TN-001

Issue: Draft A

Date: 20 June 1997

GOME Diffuser Reflectivity and Dark Signal Analysis

Author:

D. N. C. Pemberton, Serco

Reviewed:

C. Zehner, RS/PU

Authorised:

G. M. Doherty, H/RS/PM

1. Introduction

The Global Ozone Monitoring Experiment (GOME) was launched on ERS-2 in April 1995 and has been continuously operational since then. It is a scanning nadir-viewing spectrometer, with its primary scientific objective being to retrieve total column ozone globally. A more detailed description of the instrument can be found in [1]. In common with previous instruments to measure total column ozone from space such as TOMS and SBUV, it measures the back-scattered radiance from the Earth's atmosphere and surface, and the solar irradiance which is viewed via a diffuser plate to provide a reference spectrum at comparable intensity. These diffuser plates have been found to be subject to degradation (see [2] for example) particularly when subject to shorter wavelength ultra-violet light, and efforts have been made to characterize this degradation for instruments such as SBUV/2, where the diffuser plate was exposed for a total of around 750 hours between 1979 and 1986. GOME has been designed with a cover for its diffuser plate in an attempt to minimise this degradation, with exposure usually being for a short time for one orbit each day to obtain a reference solar spectrum, and characterisation of any degradation is possible by means of the on-board Pt/Cr/Ne calibration lamp. This technical note investigates to what extent, if any, GOME's diffuser plate has degraded, and to see if the measures taken have reduced the effect.

The time period for the analysis was a little more than one and a half years, using the monthly calibration data from June 1995 until January 1997. During the course of this analysis, a problem was discovered with the algorithm used for the calculation of the diffuser reflectivity, which meant that trends in the dark signal were causing difficulties in the interpretation of the reflectivity data. Consequently the two components of the dark signal were also analysed, and the results not only allowed a better understanding of the diffuser behaviour, but also provided valuable information on the detector degradation over this same period of time.

2. ESRIN QA Tools and Data Set

The main tool used for this investigation was the Extended Rascals for GOME (ERGO) system produced under ESA contract by Dornier and SRON ([3], [4]). This is a software suite designed to provide quality assurance measures about GOME on both an automatic and interactive basis.

Every month a set of calibration files are generated which contain extra information about the instrument, as obtained from the monthly calibration sequence. Amongst these are measurements of diffuser reflectivity calculated once per spectral line per channel per orbit, as obtained using an algorithm specified in [5] and updated in [6], and the two dark signal components. These algorithms are described further below in §3.

The data set consists of some 20 monthly calibration sequences which are not quite regularly spaced in time - data were unavailable for some months as well as there being a couple of occasions on which the calibration sequence was performed more frequently. The table in Appendix A gives information about the orbits available for analysis from each monthly calibration sequence.

3. Algorithm Descriptions

The algorithms used for the calculation of diffuser reflectivity and dark signal components are summarised in the following subsections.

3.1 Diffuser Reflectivity Algorithm

The algorithm used by ERGO to calculate diffuser reflectivity may be broken down into the following components:

- Find all diffuser products for an orbit
- Find all lamp products after the last diffuser product
- Ignore the first lamp products where the integration times are all minimum
- Locate the centre of each line
- Sum five pixels around this line centre
- Calculate baseline from average of the minima of ten pixels either side of the centre
- Subtract this baseline
- Normalise according to integration time
- Average the diffuser measurements
- Average the lamp measurements
- Calculate the line reflectivity as the ratio of these averages.

The wavelengths and corresponding pixel numbers of the calibration lamp lines used are shown in the tables in Appendix B. As noted previously, the algorithm as it stands yields one ratio per line per orbit, and no error information on this measurement. Some account of lamp power stability is taken by not using measurements for the first 130s after it has been switched on, thereby avoiding its power-up phase.

3.2 Dark Signal Algorithm

- Find all dark products for an orbit
- Get their corresponding integration times
- Linear fit the integration times against the dark signal, noting Band 1A integration status
- Return the offset as the fixed pattern readout noise and the gradient as the leakage current

4. Preliminary Analysis of Diffuser Reflectivity Data

A preliminary analysis was performed on the ERGO data in July to see what conclusions could be drawn from the data set as it stood at that time. It can immediately be seen (Figure 1, topmost plot) that the data come in clusters of several points, corresponding to each monthly calibration sequence. This period is not completely regular since there were occasions (March and June 1996 for example) on which more than one monthly calibration occurred, and occasionally the sequence was not performed as scheduled on the 28th of each month. The calibration is performed over the Pacific Ocean, so only the first two of the calibration orbits at most could be affected by the South Atlantic Anomaly (SAA), an area of higher than normal background radiation, and then only during the daytime when the orbit track passes through this area.

There are two measures which may be taken in an attempt to identify statistically erroneous points which can then be removed, yielding a smoother data set for further analysis. The first of these is

to obtain the mean reflectivity of all the points and discard those lying more than 3 standard deviations (SD) from the mean (see Table 1 below); the second is to analyse the spread of the points in the individual clusters and to discard those clusters where this spread is significantly (more than 2.5 SD - since we are dealing with a group of lines rather than individuals the selection criterion is stricter) greater than the others (see Table 2 below). The result of applying these transformations to the first line in channel 1 can be seen in Figure 1, where the points to be discarded are marked with a star.

Channel	Nov 95	Early Feb 96	Mar 96	Apr 96	May 96	Jun 96
One	-	-	-	-	1-7, 9, 11	3
Two	-	-	-	2-6, 8	1, 7	-
Three	6	9	-	1-4, 8, 11, 13-18	5-7, 10, 12	10
Four	1	-	20, 21	2, 4-6, 8-21	1-4, 7	1-3

Table 1: Bad Line Occurrences Listed By Line Number In Channel

Channel	Dec 95	mid Mar 96	end Mar 96	Apr 96	May 96	Jun 96
One	-	1, 8	-	-	9	5-7
Two	-	6	-	7	2, 4	1, 3, 8
Three	-	-	-	-	1, 9, 11, 13	4-7, 12
Four	21	-	16-19	2, 3, 7	8, 12	-

Table 2: Bad Cluster Occurrences Listed By Line Number In Channel

From these two tables it can be seen that there is no consistent pattern where there are problems in all channels for a particular month, except for May 1996. There are some 100 occurrences listed here, of which 40 are related to one particular orbit (5346) in April 1996. Although this orbit does pass close to the SAA, it would be unreasonable to assume that this was the cause of the bad data, since other orbits which are similarly close do not show similar behaviour. For example, orbit 4488 which is the first orbit of the calibration sequence in late February 1996 has no bad data points associated with it. Further to this, of the remaining 60 bad points only 26 occur in orbits where they might have been affected by the SAA. This result is also expected since the long integration times used for the diffuser characterisation, which would be sensitive to perturbations in the background radiation environment due to the low signal, are time-lined to occur during the nighttime part of the orbit.

Once all the data had been processed in this way, it was possible to examine dependencies of the diffuser reflectivity on wavelength (by line and by channel) and time (orbit). A surface plot for channel 1 is shown in Figure 2, where dependencies on both wavelength (higher reflectivity at shorter wavelengths) and time (reflectivity increasing with time) can be seen.

When an average is taken over wavelength for each channel, only the time dependency remains, and a straight line fit to the data gives the following table, where all reflectivity data have been multiplied by one thousand. The data are shown in Figure 3.

Channel No.	1	2	3	4
Mean	830	570	650	540
% / Year	14	-0.9	1.8	1.1

Table 3: Preliminary Diffuser Reflectivity Values * 1 000 000

The conclusions one can draw from this are rather limited, since the data are obviously still noisy, but essentially there is no discernible trend in channels 2, 3 and 4. Channel 1 however shows an increase in reflectivity of around 14% a year, with the reflectivity being higher at shorter wavelengths (as seen in Figure 2). This was rather unexpected behaviour (if anything a decrease in reflectivity at short wavelengths was predicted [2]) and so efforts were made to a) reduce the noisiness of the data, particularly for channel 1 and b) find an explanation for the observed behaviour.

5. Diffuser Reflectivity Algorithm Enhancement

Given the large number of direct lamp measurements per orbit, and the fact that several measurements via the diffuser are also made, combining these after averaging into just one ratio with no error information as was done previously is obviously resulting in some loss of information. Consequently it was decided to ratio all lamp measurements against all lamp via diffuser measurements, combining these to provide a mean and variance. This error measure then allows the measurements for individual lines to be combined in the standard way [7] which gives more weight to those with a small error *i.e.*:

$$\hat{\sigma}^2 = \left\{ \sum_{i=1}^n \sigma_i^{-2} \right\}^{-1} \quad \text{and} \quad \hat{x} = \hat{\sigma}^2 \cdot \sum_{i=1}^n x_i / \sigma_i^2$$

thus giving an optimal estimate of channel reflectivity. The effect this technique has can be seen by examining Figure 4, which shows the errors for each cluster for the individual lines of channel 1, using a different symbol for each cluster. Correlation is obviously low between error size and cluster (in each cluster one finds lines with low and high errors, and this pattern is different for each cluster), whereas it is noticeable that lines 1, 2, 3 and 6 have consistently higher errors. This means that when the data are combined to provide a channel reflectivity, these lines will provide only a very small contribution.

Figure 5 shows the behaviour with time of the reflectivity calculated for individual lines from channel 1 - the correlation between the size of the errors in Figure 4 and the reflectivity values (both absolute and trend) is immediately obvious. Consequently it is to be expected that both these values will decrease for the channel average using the above method.

The optimal estimation technique was included in an upgrade (August 1996) to the ERGO system, and all the monthly calibration data were re-processed, together with later data from July, August and September 1996. They were again filtered statistically as described above in §4 (note

that the revised algorithm makes little difference to the individual values, so the same lines were removed, but there is now an error estimate for each line). The corresponding table to that shown in the preliminary analysis section is shown below, and the data are plotted as the bottom graph in Figures 6 to 9.

Channel	1	2	3	4
Mean	620	560	540	540
% / Year	9.2	1.4	-1.7	-0.9

Table 4: Revised Diffuser Reflectivity Results * 1 000 000

Although both the noise and the size of the trend in the data for channel 1 has been reduced and brought more into line with other results, it is still significantly different and so efforts were turned towards finding an explanation for this difference

6. Dark Signal Analysis

During an early review of this document, C. Caspar (ESTEC) noted that there was a problem with the way the dark signal correction was done in the diffuser reflectivity algorithm. This is due to the use of the average of the minima on either side of the line, which results in the dark signal contribution to the total being underestimated, and the line signal overestimated. Under circumstances where the dark signal is much greater than the line signal, such as occurs when a very weak lamp line is viewed via the diffuser, it is possible for the diffuser reflectivity to be substantially overestimated. Consequently, an analysis of the dark signal was performed which allowed the effect to be quantified.

The dark signal for GOME is defined as being comprised of two parts - a constant value of between 140 and 150 binary units (BU) which is the fixed pattern readout noise (FPRN) and a time dependent component of around 2 binary units per second which is the leakage current (LC).

Results for January 1997 for two of the four channels are shown in Figure 10, using only those products where the integration is complete for all bands so as to avoid a known cross-talk problem. Immediately apparent in the FPRN is a superimposed spectral signature probably due to light reflected from a baffle when the mirror is pointing to deep space.

To investigate this further, the data were decomposed into the components from each different integration time. An example of this is shown from June 1996 for channel 4 in Figure 11. Looking at all the data, it became clear that this spectral signature is only present for integration times of 3s and 24s, where the monthly calibration sequence performs dark signal measurements in the daytime part of the orbit.

A further problem was also seen with the measurements in channel 2 at 1.5s, channel 3 at 0.375s and channel 4 at 0.09375s where a slow change in the dark signal across the detector elements is seen. The problem of some dark signal readouts being dependent on the integration status of other channels was noted in the functional performance tests performed at the TNO Institute of Applied Physics (TPD) in Holland on the breadboard model (BBM) [8]. However, the monthly calibration timeline does not vary, and so it was sufficient to identify where these effects occurred. They are shown for the example case of June 1996 in Figure 12. Consequently measurements at these problematic integration times were excluded from further trend analysis. Note that discarding the daytime measurements removes any potential problems from South Atlantic anomaly effects, since

the nighttime monthly calibration measurements occur well away from this area.

The analysis of the remaining data was performed by taking the middle file of each monthly calibration sequence, calculating the gradient (LC) first from all valid integration times, and then using this to extrapolate from the shortest integration time to get the offset (FPRN). Trends were calculated for both the FPRN and the LC, and for the noise on these measurements. The results are shown in Table 1 below.

Ch.	FPRN	Noise	LC	Noise
1	+0.6	+5.4	+13.3	+34
2	+1.2	+14.9	+14.9	+35
3	+0.3	+8.6	+13.5	+33
4	+0.6	+2.3	+17.8	+88

Table 5: GOME Dark Signal Trends; % per year

From this one can conclude that there is no significant change in the fixed pattern readout noise, but that a linear increase in the leakage current is seen, which is also becoming noisier with time.

7. Impact of Dark Signal Trends on Diffuser Reflectivity Analysis

To calculate the impact of the dark signal trends, the dark signal measurements were analysed at the positions of all the lamp lines used for diffuser characterisation, and the values of the mean - minimum difference calculated for each monthly calibration sequence. These values were then used to adjust the lamp measurements via the diffuser, and the reflectivity values recalculated, neglecting data from lines so weak that they were less than the dark signal + 3SD. In the table below are shown the data for the lines in channel 1, and it can be seen immediately that the effect of the dark signal trend is to cause both the absolute values of all lines viewed via the diffuser, and the trends therein, to be overestimated.

Line	Approx. Intensity (BU)	Annual Change Mean - Min	Apparent Intensity Change	Start / End Mean - Min		Intensity Overest. Start	Intensity Overest. End
1	40	10	25%	23	36	58%	90%
2	85	16	19%	19	46	23%	54%
3	75	15	20%	24	49	32%	65%
4	190	16	8%	20	40	11%	21%
5	120	14	12%	19	38	16%	32%
6	55	3	5%	22	21	40%	38%
7	205	9	4%	19	35	9%	17%
8	230	14	6%	18	41	8%	18%

Line	Approx. Intensity (BU)	Annual Change Mean - Min	Apparent Intensity Change	Start / End Mean - Min		Intensity Overest. Start	Intensity Overest. End
9	375	8	2%	29	44	8%	12%
10	1000	20	2%	15	49	2%	5%
11	445	9	2%	23	32	5%	7%

These corrections were performed to all the data used, and the diffuser reflectivity values recalculated. The results and the zero change lines are shown in Figure 13. On these plots are also shown the errors associated with each point (3 SD, and quite large since they involve the combining of the diffuser measurement errors with those for the dark signal), and it can be seen that the small value of the trends, which are linear best fits weighted by the measurement precision, are well within the bounds of zero change.

8. Comparison with Other Results

TPD and ESTEC presented their results at the GOME QA workshop held at ESRIN (Frascati, Italy) in early September 1996. Their values, reproduced with permission, are given in the table below and, together with the ESRIN results *after* dark signal correction all given to two significant figures. The margins given on the % / year figure are 1 SD in the straight line fitting coefficients and are as plotted in Figures 6 to 9, except for the ESRIN data which are those as shown in Figure 13 (after dark signal correction). Note that in these plots the x axis is in days since launch for TPD and ESTEC, and orbits since launch for ESRIN.

Ch	Mean			SD			% / Year		
	TPD	ESRIN	ESTEC	TPD	ESRIN	ESTEC	TPD	ESRIN	ESTEC
1	570	570	590	30	14	12	25±16	-3.0±1.0	-2.0±0.5
2	520	520	500	20	14	9	19±9	1.0±0.5	2.5±0.5
3	470	520	480	30	9	5	6±16	0.0±2.0	0.5±0.5
4	540	530	540	20	4	5	-1±8	0.0±0.5	0.5±0.5

Table 6: Comparison of Diffuser Reflectivity Results * 1 000 000

Comparing these results it can be seen that there are the greatest margins on the TPD data set which is due partly to the fact that it contains fewer (6) samples. The larger margins on the ESRIN data set are for the reasons given at the end of section 7. It can be seen that agreement is generally good, particularly between the ESRIN and ESTEC data sets which cover a much longer period than that of TPD.

9. Summary

GOME diffuser reflectivity data as calculated using the ERGO algorithm are inherently noisy. Optimal estimation as described above provides a good way to combine them, making full use of the data available at ESRIN. Channels 2, 3 and 4 show insignificant changes over the 8000+ orbits for which they have been monitored at ESRIN, and agreement with results from TPD and ESTEC is good for these channels.

Channel 1 showed a significant increase in diffuser reflectivity, but this was shown to be due to a weakness in the ERGO algorithm. It affected Channel 1 predominantly since there are many weak lamp lines used in this region for diffuser characterisation.

Trends in the dark signal were investigated and shown to be capable of explaining all apparent trends in diffuser reflectivity.

10. Conclusions and Recommendations

Over a period of more than eighteen months, the following conclusions regarding trends in the GOME dark signal and diffuser reflectivity have been reached.

- No significant change is seen in the fixed pattern readout noise
- There is an increase of ~15% per year in leakage current for all detectors
- Leakage current measurements are becoming much noisier with time
- No significant change is seen in the diffuser reflectivity in any channel

These results, from in-flight measurements, can be utilised to predict the likely degradation which will be encountered in missions with similar components, such as SCIAMACHY. One can further conclude that the measures taken to protect GOME's diffuser plate from degradation have been successful so far, with no significant reflectivity change having occurred.

It is recommended that the ERGO system calculate the dark signal separately from the monthly calibration files, and use this for a proper dark signal correction of the diffuser. If this proves impossible, significant improvement would still be gained by using only the strongest lines for the calculation, since this is where the impact of the dark signal trend is least. An alternative method would be to include a parameterisation of the dark signal behaviour based on the results of this analysis, and to use this to correct the results produced by the existing algorithm, though this approach would be the least satisfactory. It is not possible to make a satisfactory dark signal correction based on measurements made whilst the lamp is on.

11. Acknowledgements

Thanks are due to the GOME team at ESTEC, in particular C. Caspar, for reviewing an earlier version of this document and providing valuable input.

Thanks are also due to the other members of the ESRIN GOME team (A. Dehn, R. Koopman, M. Suttie, C. Zehner) and T. Hermsen for help in reviewing this document and assistance in the re-processing of the monthly calibration data using the ERGO system.

12. References

- [1]: GOME User's Manual SP-1182
ESA Publications Division September 1995.
- [2]: Report of the International Ozone Trends Panel
WMO Report No. 18 Vol. 1, §2.3.6 1988.
- [3]: ERGO Software User's Manual
DOR-GO-QA-SUM Issue 1.0 12/12/1995
- [4]: ERGO Design Document
DOR-GO-QA-DD Issue 2.0 12/12/1995
- [5]: GOME Data QA - Specification of Instrument Parameters - S. Slijkhuis
SRON-GOME-QA-TN01 Issue 2/A 30/06/1995.
- [6]: ERGO Test Report of Final S/W Delivery Dec-1995 - S. Slijkhuis
SRON-GOME-QA-TN04 Issue 1 09/02/1996.
- [7]: Remote Sounding of Atmospheres by J.T. Houghton, F.W. Taylor and C.D. Rodgers
Cambridge University Press 1st Edition 1986.
- [8]: Functional / Performance Test on GOME BBM - Olij, C. & Zoutman, A. E.
TPD-ERS-GO-MIR-11 Issue 2 1993

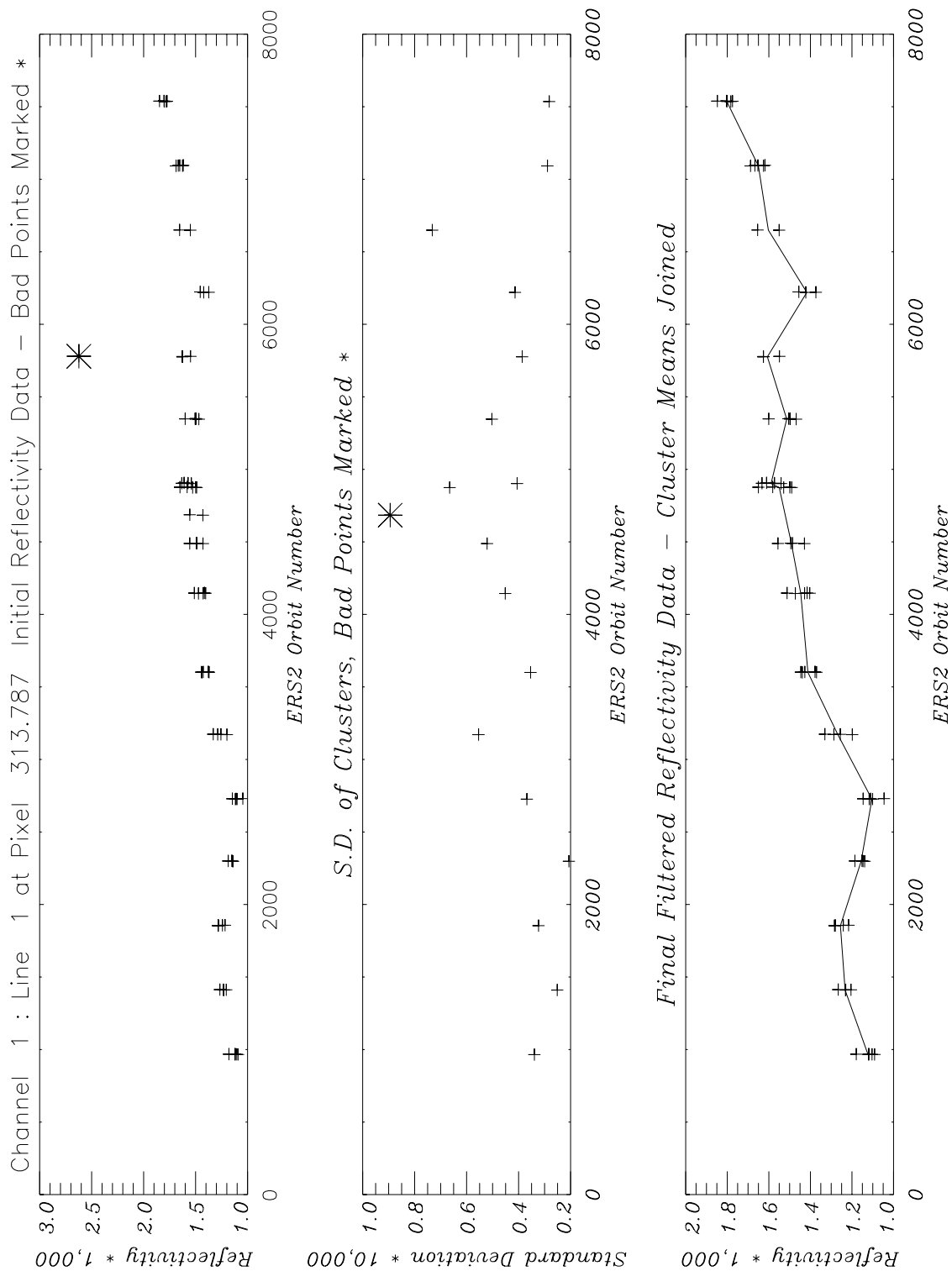


Figure 1. Statistical Filtering of Data from First Line in Channel 1

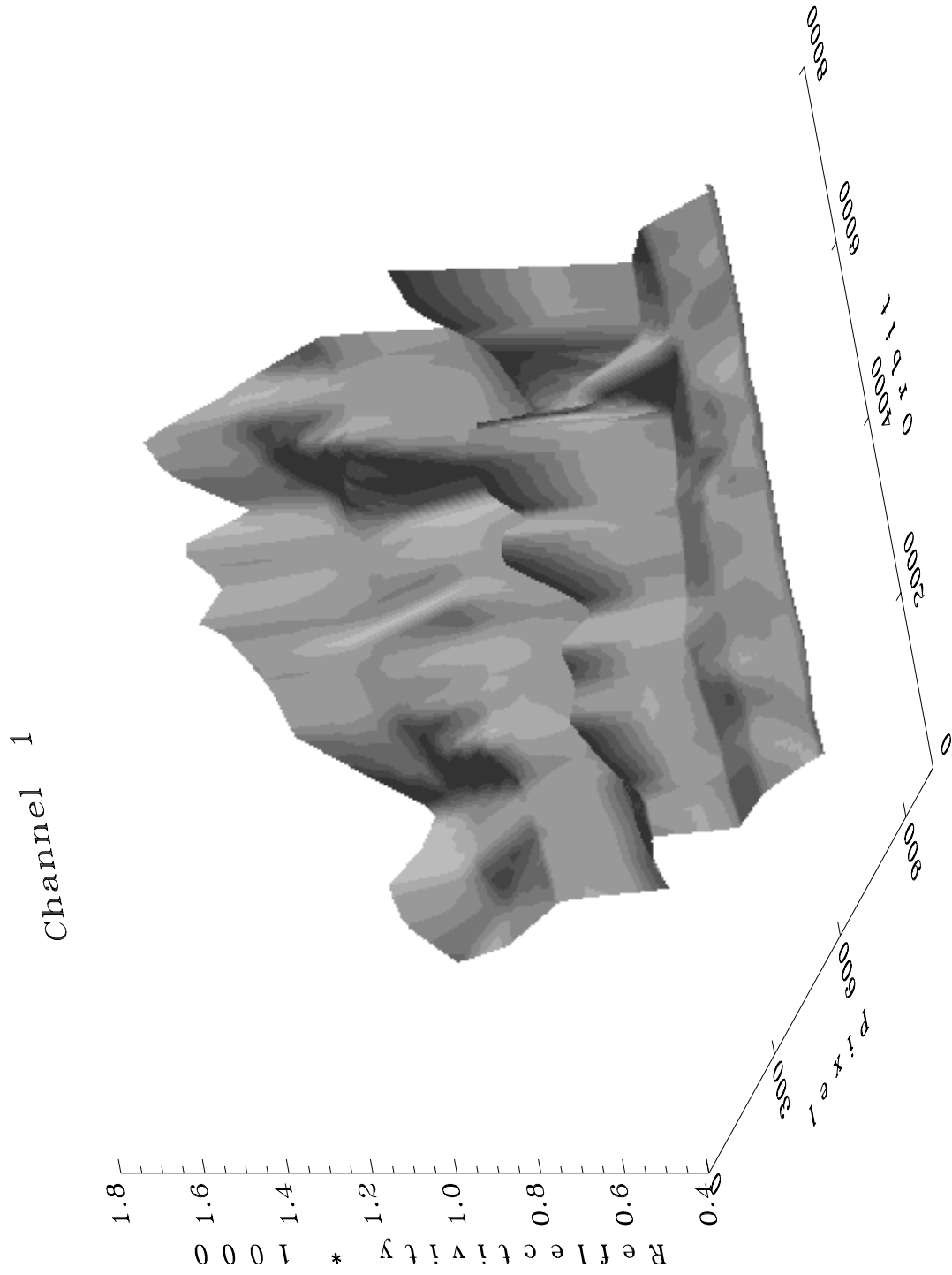


Figure 2. Surface Plot of Channel 1 Reflectivity Data

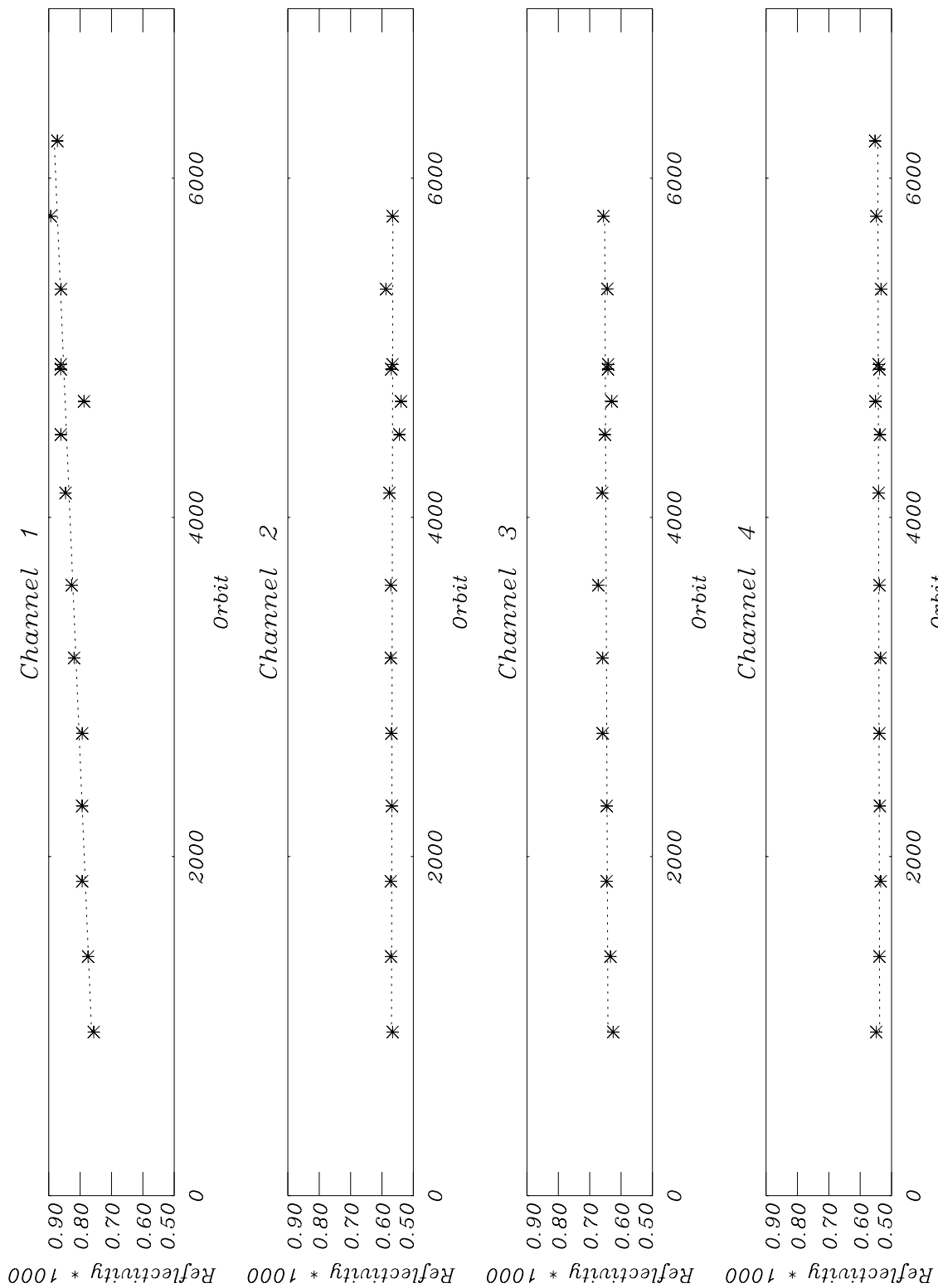


Figure 3. Preliminary Results for Mean Channel Reflectivity

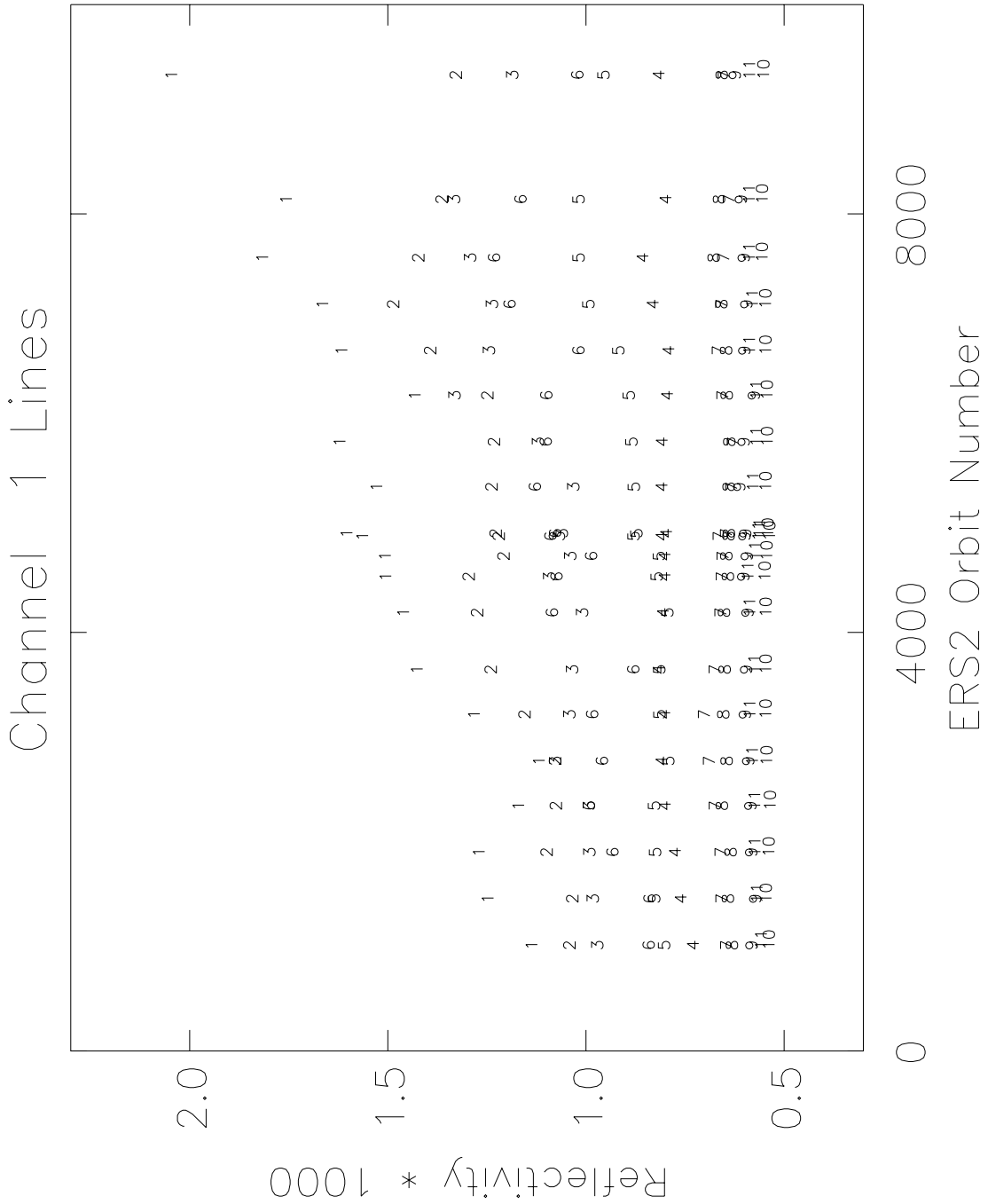


Figure 5. Behaviour over Time for All Lines of Channel 1
(the numerals correspond to those in Appendix B)

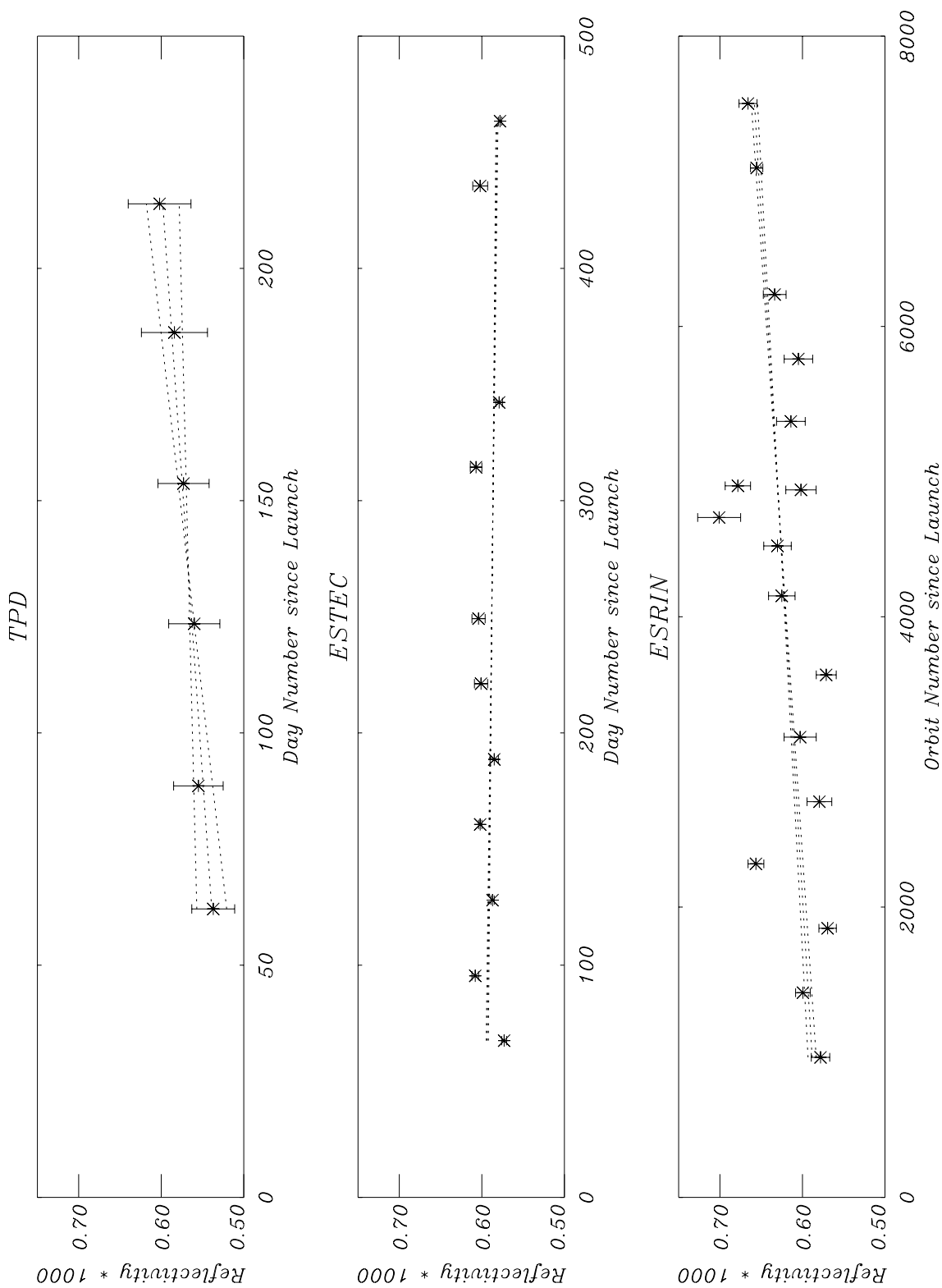


Figure 6. Channel 1 Reflectivity Comparison - No Dark Signal Correction for ESRIN Data

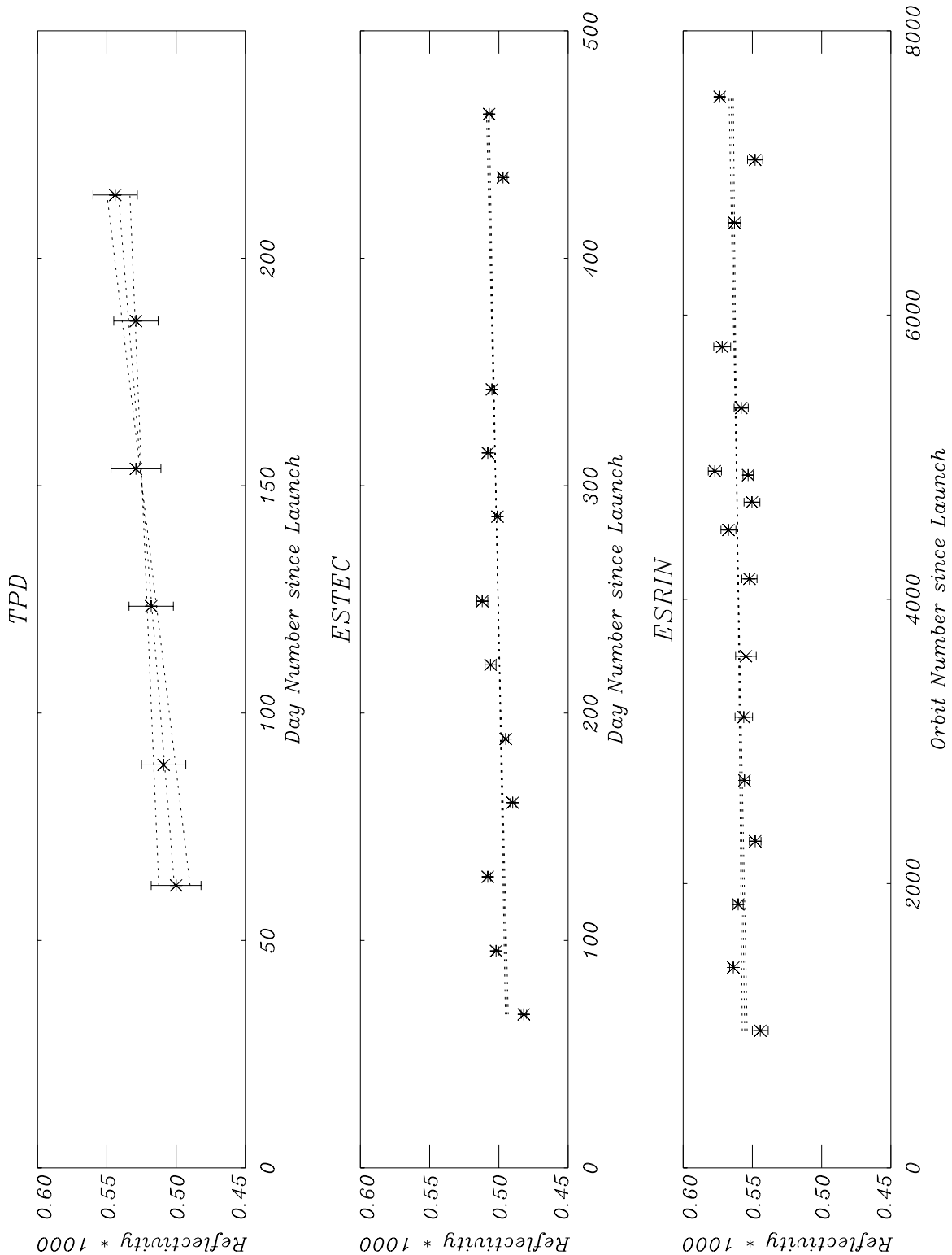


Figure 7. Channel 2 Reflectivity Comparison - No Dark Signal Correction for ESRIN Data

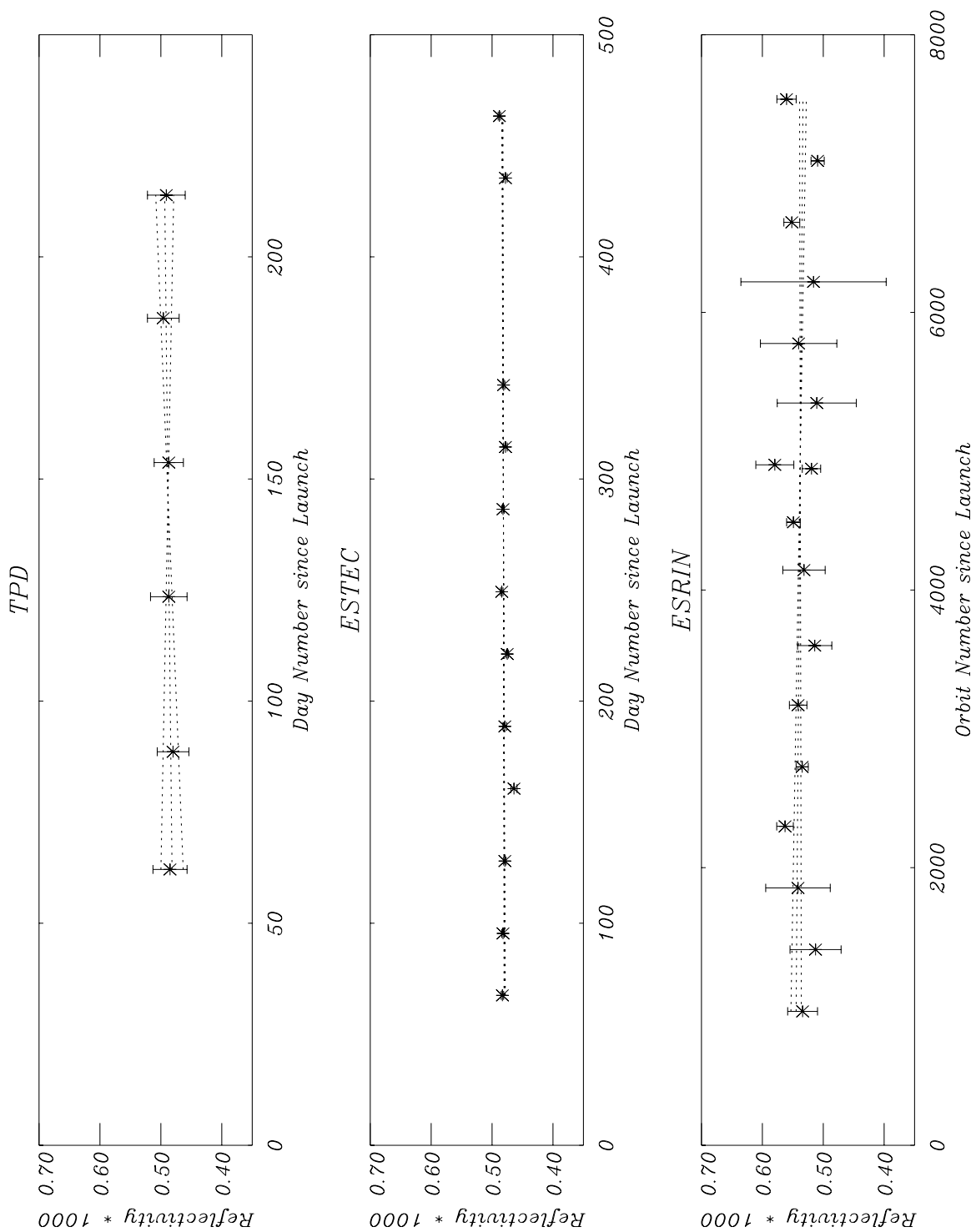


Figure 8. Channel 3 Reflectivity Comparison - No Dark Signal Correction for ESRIN Data

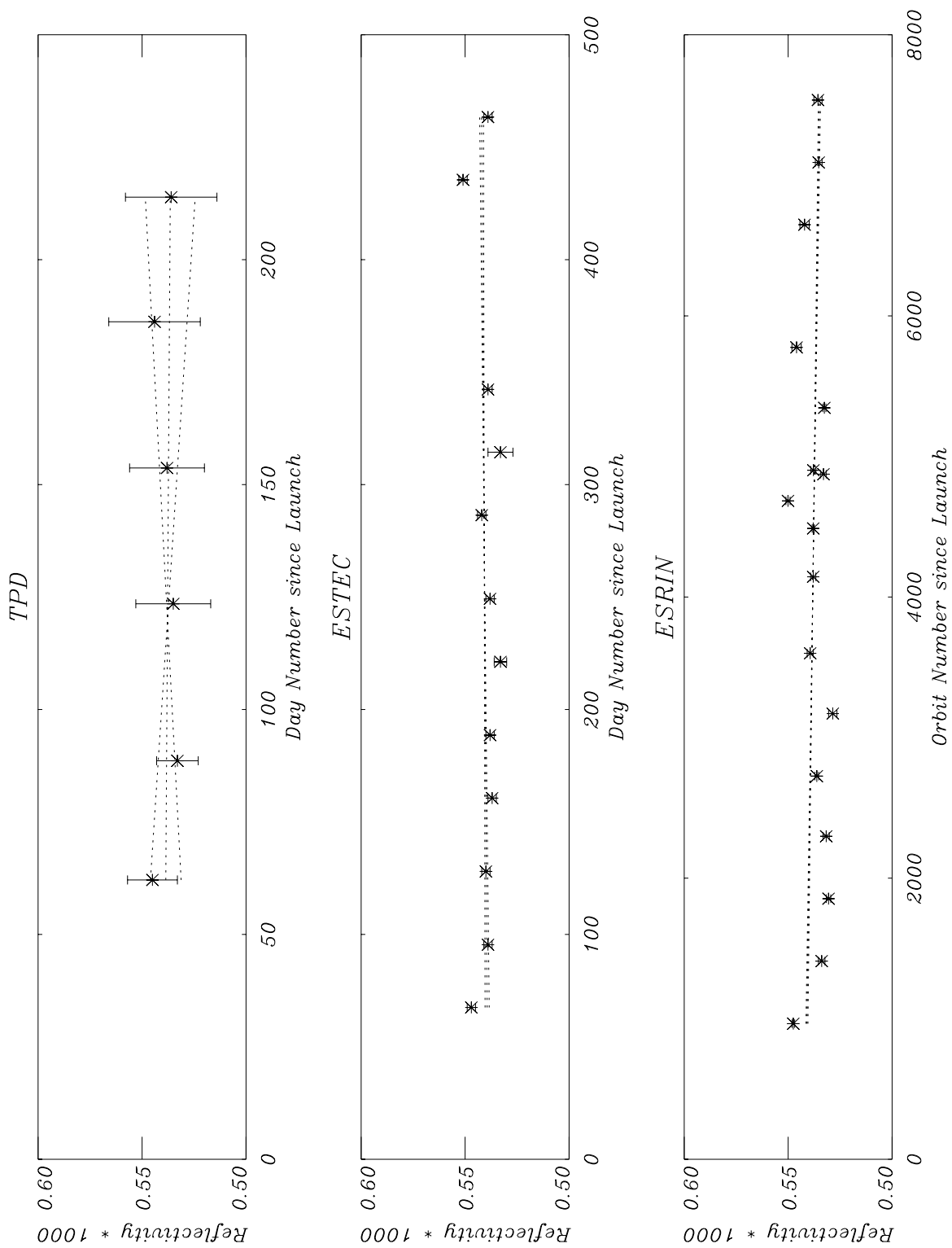


Figure 9. Channel 4 Reflectivity Comparison - No Dark Signal Correction for ESRIN Data

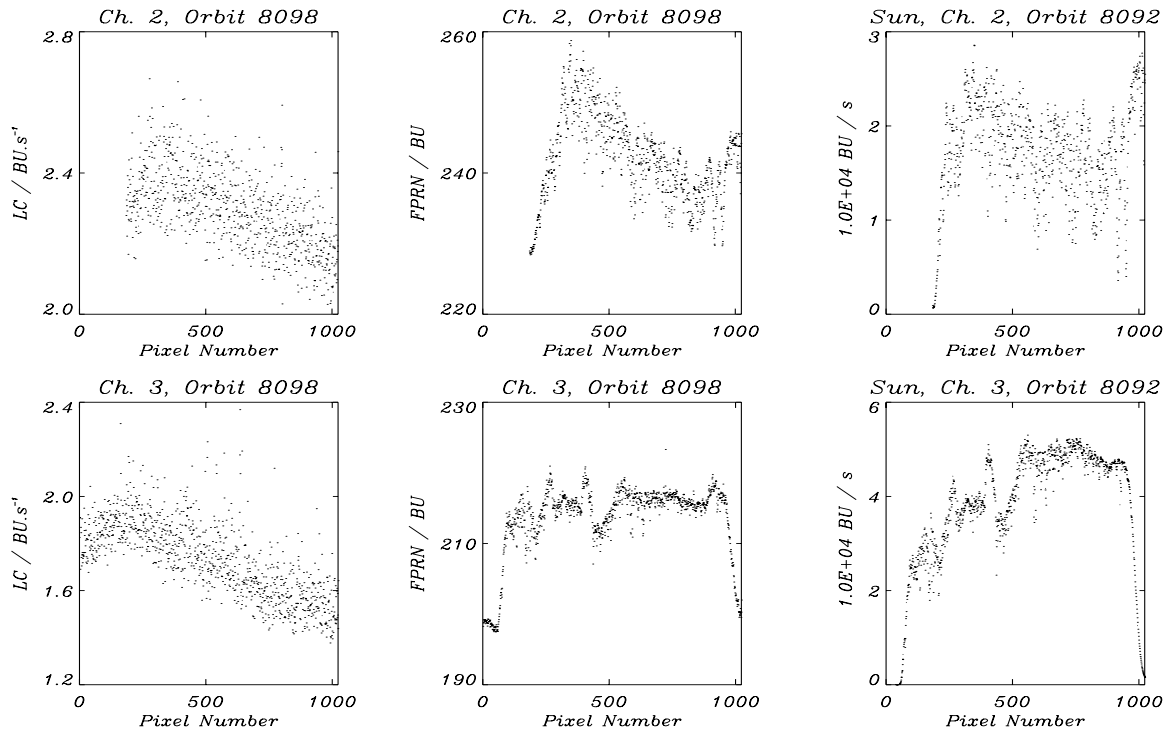


Figure 10: ERGO Dark Signal and Solar Spectrum, January 1997

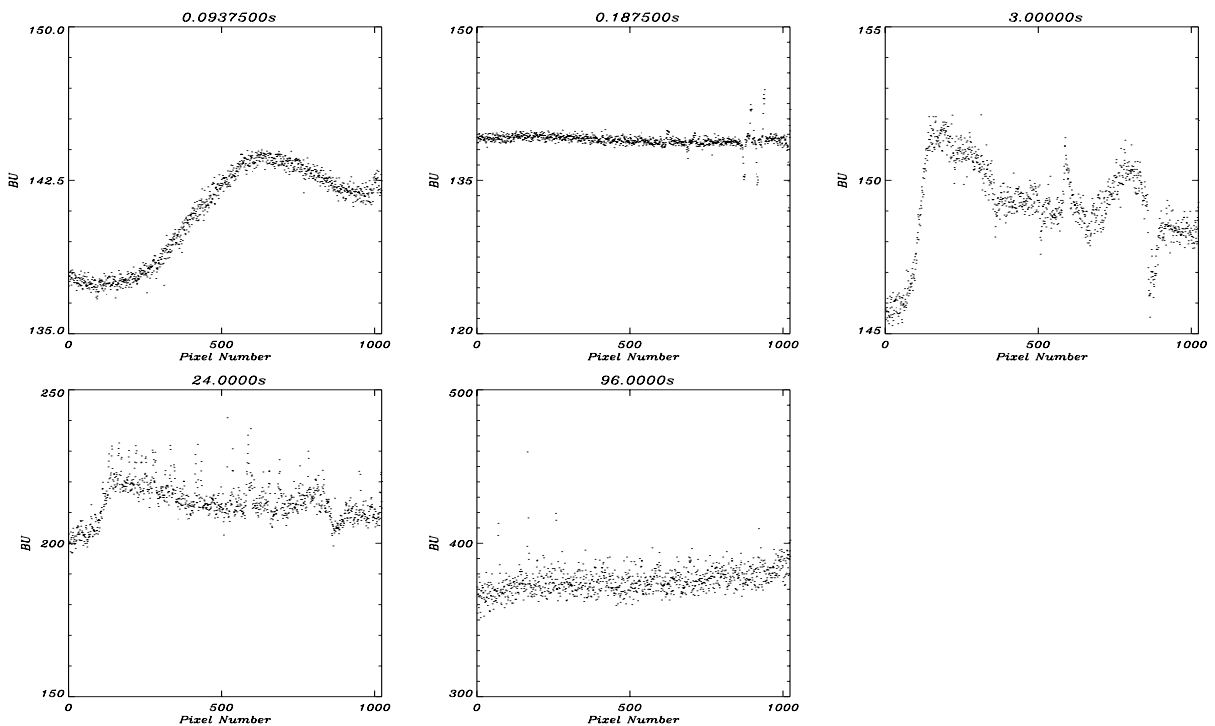


Figure 11: Dark Signal Measurements for Channel 4, June 1996

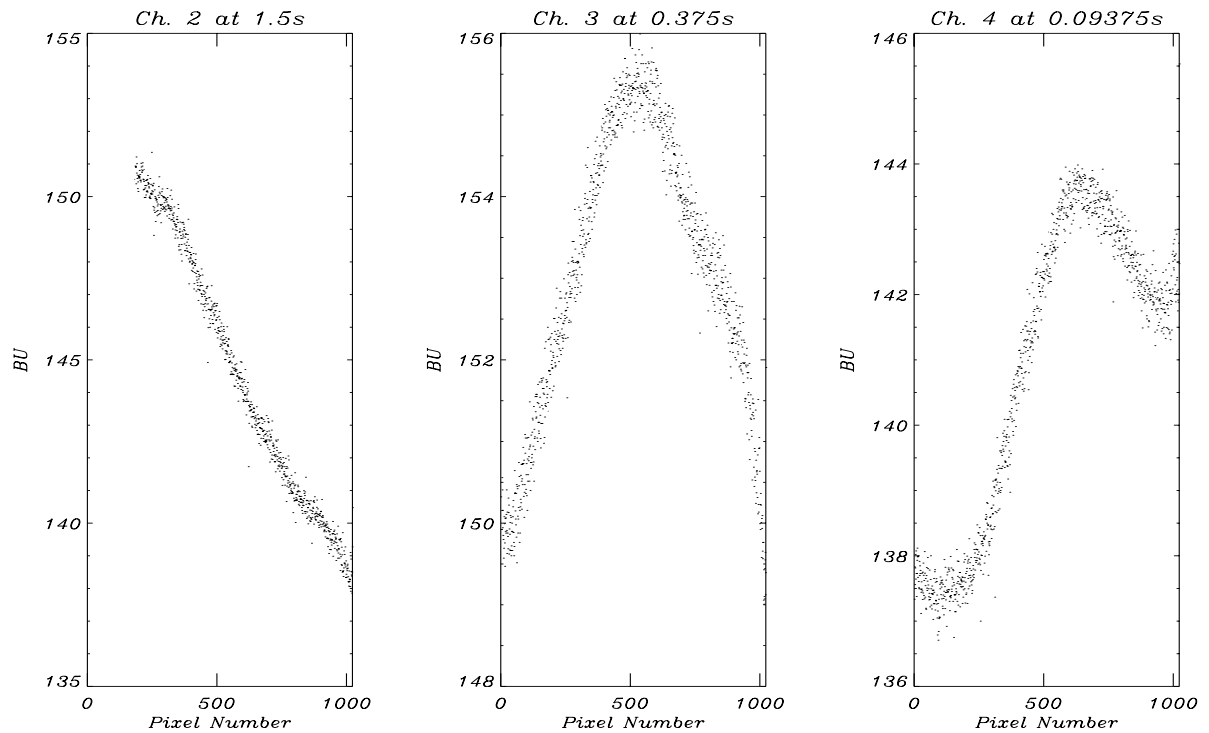


Figure 12: Integration Times and Channels where Variation of Dark Signal Across Detector Elements is Seen

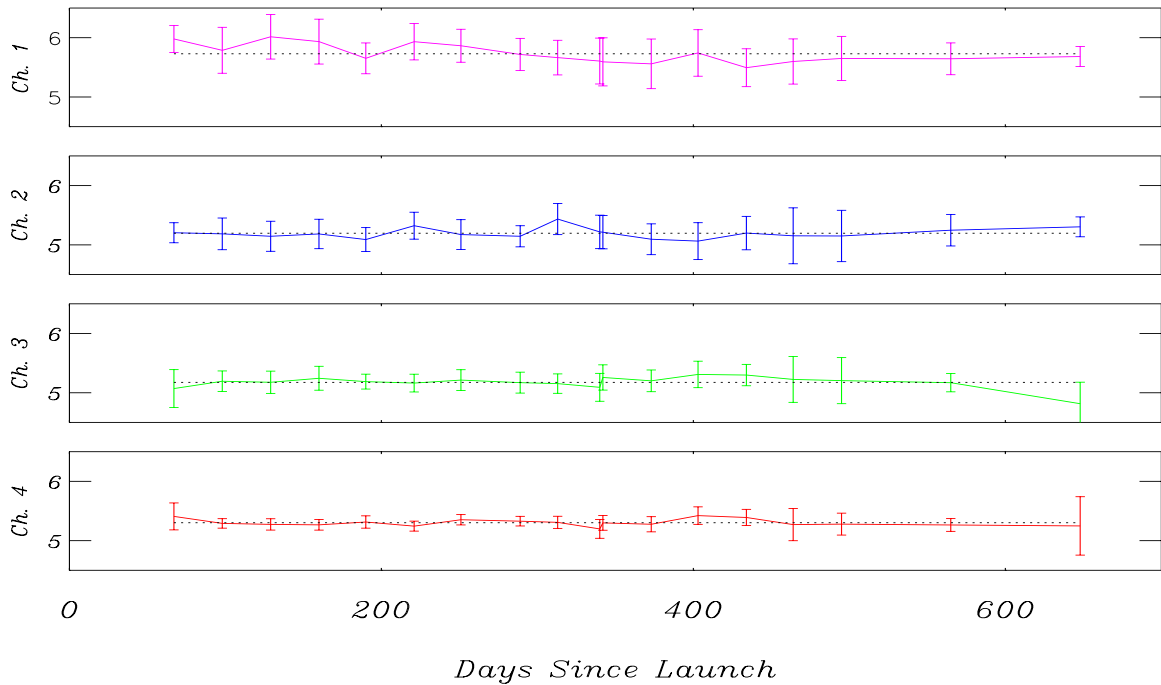


Figure 13: Diffuser Reflectivity (x 10,000) for all Channels, Dark Signal Correction Applied

Appendix A

Monthly Calibration Data Sets

Calibration Sequence	Date	Days From Launch	Orbits (No.)
1	27 June 1995	67	965 - 967; 969 (4)
2	28 July 1995	98	1410 - 1413 (4)
3	28 August 1995	129	1854 - 1857 (4)
4	28 September 1995	160	2298 - 2301 (4)
5	28 October 1995	190	2726 - 2730 (5)
6	28 November 1995	221	3171 - 3174 (4)
7	28 December 1995	251	3600 - 3604 (5)
8	04 February 1996	289	4144 - 4148 (5)
9	28 February 1996	313	4488 - 4491 (4)
10	13 March 1996	327	4684; 4687 (2)
11	26 March 1996	340	4874 - 4878 (5)
12	28 March 1996	342	4902; 4904 - 4906 (4)
13	28 April 1996	373	5347 - 5350 (4)
14	28 May 1996	403	5776 - 5780 (5)
15	28 June 1996	434	6220; 6221; 6223 (3)
16	28 July 1996	464	6649; 6650 (2)
17	28 August 1996	495	7092 - 7096 (5)
18	28 September 1996	526	7536 - 7540 (5)
19	06 November 1996	565	8094 - 8098 (5)
20	28 January 1997	648	9282 - 9286 (5)

Appendix B

Lamp Lines Used For Diffuser Calibration

Channel 1				Channel 2		
Line Number	Wavelength / nm	Pixel Number		Line Number	Wavelength / nm	Pixel Number
1	244.08	313.79		1	321.91	275.71
2	248.79	353.41		2	332.47	368.00
3	262.88	475.23		3	337.92	415.96
4	266.02	503.16		4	352.15	542.43
5	273.48	569.93		5	369.53	698.64
6	281.03	638.76		6	372.82	728.42
7	283.11	657.69		7	390.99	893.48
8	293.06	749.28		8	392.03	903.05
9	299.88	812.66				
10	304.35	854.03				
11	306.56	874.64				

Channel 3				Channel 4		
Line Number	Wavelength / nm	Pixel Number		Line Number	Wavelength / nm	Pixel Number
1	425.55	145.6		1	588.35	44.42
2	427.60	155.2		2	594.65	72.22
3	429.09	162.2		3	597.72	85.92
4	437.25	200.6		4	603.17	109.43
5	460.20	309.8		5	607.60	130.53
6	492.36	464.5		6	609.79	140.45
7	503.92	520.3		7	613.01	155.21
8	540.21	694.7		8	616.53	171.30

Channel 3				Channel 4		
Line Number	Wavelength / nm	Pixel Number		Line Number	Wavelength / nm	Pixel Number
9	556.43	772.0		9	621.90	196.02
10	574.99	859.4		10	626.82	218.84
11	576.60	866.8		11	630.65	236.66
12	580.61	885.5		12	638.47	273.25
13	582.18	892.7		13	653.47	344.13
14	588.35	921.3		14	660.08	375.64
15	594.65	950.4		15	668.01	413.61
16	597.72	964.1		16	693.14	534.83
17	603.17	988.6		17	717.59	653.62
18	607.60	1008.5		18	724.72	688.28
				19	744.09	782.40
				20	749.09	806.62
				21	753.79	829.28